2020

Acoustic space occupancy: Combining ecoacoustics and lidar to model biodiversity variation and detection bias across heterogeneous landscapes

Danielle I. Rappaport

J. Andrew Royle

Douglas C. Morton

Ecological Indicators 113 (2020) 106172

Contents lists available at ScienceDirect

Ecological Indicators

journal homepage: www.elsevier.com/locate/ecolind

Acoustic space occupancy: Combining ecoacoustics and lidar to model biodiversity variation and detection bias across heterogeneous landscapes

Danielle I. Rappaport[a,*], J. Andrew Royle[b], Douglas C. Morton[c]

[a] Department of Geographical Sciences, University of Maryland, 1149 Lefrak Hall, College Park, MD 20742, United States
[b] USGS Patuxent Wildlife Research Center, 12100 Beech Forest Road, Laurel, MD 20708, United States
[c] NASA Goddard Space Flight Center, Greenbelt, MD 20771, United States

ARTICLE INFO

Keywords:
Airborne lidar
Bioacoustics
Biodiversity monitoring
Imperfect detection
Passive acoustic monitoring
Tropical forest structure
Forest degradation

ABSTRACT

There is global interest in quantifying changing biodiversity in human-modified landscapes. Ecoacoustics may offer a promising pathway for supporting multi-taxa monitoring, but its scalability has been hampered by the sonic complexity of biodiverse ecosystems and the imperfect detectability of animal-generated sounds. The acoustic signature of a habitat, or soundscape, contains information about multiple taxa and may circumvent species identification, but robust statistical technology for characterizing community-level attributes is lacking. Here, we present the Acoustic Space Occupancy Model, a flexible hierarchical framework designed to account for detection artifacts from acoustic surveys in order to model biologically relevant variation in acoustic space use among community assemblages. We illustrate its utility in a biologically and structurally diverse Amazon frontier forest landscape, a valuable test case for modeling biodiversity variation and acoustic attenuation from vegetation density. We use complementary airborne lidar data to capture aspects of 3D forest structure hypothesized to influence community composition and acoustic signal detection. Our novel analytic framework permitted us to model both the assembly and detectability of soundscapes using lidar-derived estimates of forest structure. Our empirical predictions were consistent with physical models of frequency-dependent attenuation, and we estimated that the probability of observing animal activity in the frequency channel most vulnerable to acoustic attenuation varied by over 60%, depending on vegetation density. There were also large differences in the biotic use of acoustic space predicted for intact and degraded forest habitats, with notable differences in the soundscape channels predominantly occupied by insects. This study advances the utility of ecoacoustics by providing a robust modeling framework for addressing detection bias from remote audio surveys while preserving the rich dimensionality of soundscape data, which may be critical for inferring biological patterns pertinent to multiple taxonomic groups in the tropics. Our methodology paves the way for greater integration of remotely sensed observations with high-throughput biodiversity data to help bring routine, multi-taxa monitoring to scale in dynamic and diverse landscapes.

1. Introduction

Biodiversity loss as a direct and indirect result of human activity represents a major threat to life on Earth (e.g., Cardinale et al., 2012). Operational capacity to monitor known biodiversity is extremely limited, resulting in incomplete species inventories (Troudet et al., 2017) and sparse data coverage (Meyer et al., 2015). There is broad international interest in improving biodiversity monitoring, including efforts by the Group on Earth Observations Biodiversity Observation Network (GEO BON) to harmonize biodiversity measurements across space and time as essential biodiversity variables (EBVs). The success of EBVs for expanding the scope of routine monitoring fundamentally depends on advances in distributed monitoring technology with increased taxonomic coverage, including DNA metabarcoding, camera traps, and ecoacoustic surveys. Since most of Earth's taxonomic diversity is not visible from air or space, such high-throughput biodiversity observations may complement spatially extensive Earth observations to monitor biodiversity trends at policy-relevant extents (Bush et al., 2017). Scaling up biodiversity observations on the level needed to support global conservation commitments will also require advances in computational methods designed to adjust for data sparsity and other sampling artifacts that could otherwise confound estimates of biodiversity trends.

Strategies for routine monitoring of biodiversity confront a range of

* Corresponding author.
E-mail address: drappap@umd.edu (D.I. Rappaport).

https://doi.org/10.1016/j.ecolind.2020.106172
Received 20 March 2019; Received in revised form 12 December 2019; Accepted 31 January 2020
Available online 15 February 2020
1470-160X/

trade-offs related to taxonomic coverage and sampling bias. The existing body of biodiversity data is strongly skewed towards popular taxa (e.g. plants, vertebrates), resulting in data gaps for invertebrates and other organisms (Troudet et al., 2017). These data disparities also reflect limitations in taxonomic expertise, especially in biodiverse tropical forests, which harbor over 50% of Earth's species, many of which are not readily identifiable. Even birds, the most well-studied taxa, suffer from high rates of imperfect detection and species classification errors in tropical forests, where over 95% of individuals are heard but not seen by surveyors tasked with discriminating among hundreds of species with rich vocal repertoires in dark forest understories (Robinson et al., 2018). Additionally, there is seldom enough information about species distributions to establish sampling protocols that account for key sources of sample bias from spatial variability and habitat heterogeneity, especially in tropical forests where visibility is limited, canopy structure is complex, and extents are large.

Emerging remote sensing tools, such as lidar and ecoacoustics, may support goals to expand the scope of biodiversity monitoring by collecting biodiversity variables across taxonomic, spatial, and temporal domains in a cost-effective and non-invasive manner. Lidar, short for Light Detection and Ranging, provides detailed, three-dimensional (3D) information on habitat structure, and lidar-derived measures of forest structure have been used to assess patterns of species diversity and abundance in forested environments (e.g., Goetz et al., 2007; Bergen et al., 2009). High-density airborne lidar data capture fine-scale changes in forest structure from human activity, with 3D data over hundreds to thousands of hectares needed to support landscape-scale investigations (Longo et al., 2016; Rappaport et al., 2018). Ecoacoustic surveys offer a complementary perspective by providing direct observations of the animal community over diurnal, seasonal, and interannual time scales. Remote acoustic surveys have the potential to track many animal taxa (e.g. birds, amphibians, insects, mammals, bats), and, unlike traditional field methods (e.g. point-counts), the acoustic environment can be surveyed simultaneously at multiple sites with concurrent recorders covering large spatial extents (Gibb et al., 2019). These remote sensing tools have been used independently for biodiversity monitoring, but they have rarely been used together, despite known associations between habitat structure, habitat use, and acoustic signal transmission (Pekin et al., 2012; Royle, 2018).

Three primary developments are needed to enable widespread use of ecoacoustics for routine biodiversity monitoring. First, acoustic analysis techniques that derive information about multiple taxa while bypassing the need for species identification are critical to enable rapid, replicable, and scalable assessments of biodiversity change. The sonic signature of a site, or "soundscape," encodes information about the resident animal community, and the 3D structure of the soundscape defined by time, frequency, and amplitude represents a valuable opportunity to capture multiple taxa. As taxonomic groups emit acoustic signals (vocalizations, stridulations) at routine periods of the day and at standard frequency ranges, the soundscape can be regarded as an abstracted representation of the animal community, comprised of acoustic transmission channels in time–frequency space that are occupied by distinct species composites (Aide et al., 2017).

Second, analytic methods are needed to handle the data complexity of soundscapes from biodiverse environments in a manner that is robust across time scales, sensors, and acoustic conditions (Gibb et al., 2019). A diversity of acoustic indices have been developed by collapsing the 3D soundscape into measures of energy distribution along either the time or frequency dimensions, but seldom both (as reviewed by Sueur et al., 2014). Such indices have been used to predict species richness in low-diversity temperate ecosystems dominated by a single vocal taxon, but predictive performance has been less stable in tropical forests, which are characterized by diverse signaling assemblages, multi-taxa choruses, and constant background noise (e.g. routine rainfall, insect stridulations) (Eldridge et al., 2018). Retaining the time and frequency dimensions may be crucial for capturing the complex patterns of acoustic energy in biodiverse tropical systems (Eldridge et al., 2016, 2018; Aide et al., 2017). Furthermore, preserving the spectral-temporal structure of soundscapes is conceptually consistent with the hypothetical link between biodiversity and acoustic diversity, originally introduced in the Acoustic Niche Hypothesis (ANH; Krause, 1987). The ANH purports that acoustic space is partitioned into spectral-temporal 'niches' through evolutionary processes and competitive interactions that minimize signal overlap among co-existing species. Whether taxa do in fact occupy coherent acoustic niches is an area of active research, and, while much remains to be learned about the factors that structure acoustic transmission space (Pijanowski et al., 2011), the proportion of that space occupied by biota has been found to be an effective proxy for species richness in tropical forests (Aide et al., 2017). Exploiting this spectral-temporal structure—referred to henceforth as "acoustic space occupancy"— may open up new analytic pathways for rapid and replicable assessments of biodiversity.

Third, statistical solutions must be developed to account for observation bias in soundscape recordings. The likelihood of detecting a soniferous species occupying a site depends not only on whether it is acoustically active during a given survey, but also on a myriad of factors that influence the detectability of its acoustic signals, such as interference with vegetation, obfuscating abiotic noise, signal amplitude and frequency, distance of the animal to the recorder, micrometeorology, and survey effort, among others (Wiley and Richards, 1982). Nonetheless, most soundscape analysis methods do not adjust for sampling artifacts and detectability, despite the fact that imperfect detection can skew ecological inferences (Royle, 2018). For example, vegetation selectively limits the propagation of certain frequencies due to the physics of sound attenuation in forested environments (Wiley and Richards, 1982), so unless properly addressed by statistical methods, raw soundscape observations are likely to underestimate the extent of occupied acoustic space in dense forest habitats.

Here, we accommodated these three methodological objectives using a novel analytic framework for capturing signals relevant to multiple taxa while accounting for sources of detection bias in remote audio surveys. Our methodological approach, the Acoustic Space Occupancy Model (ASOM), assumes that the observed soundscape is not a perfect characterization of the acoustic community, and therefore the modeling framework reconstructs the true, latent soundscape in a manner that is directly analogous to the 'occupancy model' framework for estimating species occurrence probability (e.g. MacKenzie et al., 2002). ASOM is a hierarchical model with explicit covariate effects to separate the ecological process (i.e., acoustic space occupancy) from the observation process (i.e., acoustic space detection) and quantify parameter uncertainties. Furthermore, its flexible framework can accommodate a range of extensions and study designs (MacKenzie et al., 2018).

We applied ASOM to ecoacoustic and airborne lidar data from a frontier forest mosaic in the southern Brazilian Amazon to illustrate the utility of our model and investigate hypothesized synergies between 3D observations of acoustic space-filling and physical space-filling. The enormous structural diversity of the study region represents a valuable test case for evaluating the role of forest structure in explaining variability in acoustic community assembly between sites and informing models of detection failure.

2. Materials and methods

2.1. Case study region

We collected ecoacoustic and lidar data in the municipalities of Nova Ubiritã and Feliz Natal, Mato Grosso, near the southern extent of closed-canopy forests in the Brazilian Amazon (Fig. 1). More than 40 years of agricultural expansion, selective logging, and understory fires have given rise to a mosaic of fragmented and degraded forests with a diversity of canopy structures (Rappaport et al., 2018). The non-

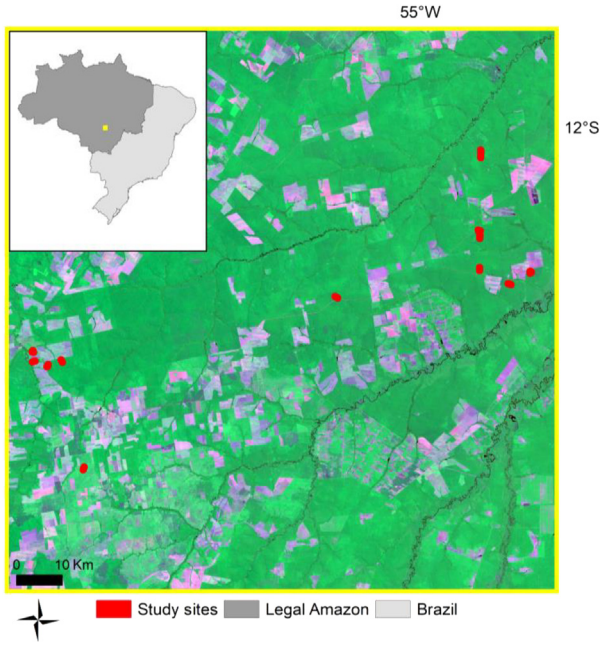

Fig. 1. The locations of the ecoacoustic and lidar surveys (red polygons; n = 34) shown in relation to the case study landscape (2014 Landsat composite, bands 543) and broader regional context (map inset).

forest matrix is dominated by large-scale commodity agriculture, including soy, corn, and cattle ranching. The largest area of intact forest remaining in the region is in the adjacent Xingu Indigenous Park; airborne lidar acquisitions include intact forest areas for reference.

2.2. Lidar surveys and analysis

High-density airborne lidar surveys (≥14 returns per m^2) were conducted by the Sustainable Landscapes Brazil project between 2013 and 2016 to target a range of intact and degraded forest conditions in the region. Within the lidar coverage, 34 sites (forest patches ≥ 300 m in radius) with uniform degradation history were identified (Rappaport et al., 2018). Sites were spaced at least 300 m from one another and from the non-forest matrix to avoid edge effects and establish spatial independence (Fig. 1). Standard lidar metrics were calculated for each site following methods developed for NASA Goddard's Lidar, Hyperspectral, and Thermal (G-LiHT) Airborne Imager (Cook et al., 2013; Table 1), and biomass was estimated using a regional lidar-biomass model based on mean top of canopy height (Longo et al., 2016).

2.3. Acoustic surveys and analysis

We deployed passive acoustic recording sensors at the center of each site to survey the spatiotemporal patterns of acoustic communities between August and October 2016. ARBIMON acoustic sensors (Aide et al., 2013) were installed at breast height (1.37 m) to record all activity between 0 and 22 kHz. The acoustic environment was sampled for one minute every five minutes for a minimum of five days at each site, totaling more than 1100 h of acoustic survey data.

Three preprocessing steps were used to convert the recording archive into soundscape matrices of acoustic space use following previous methods (Aide et al., 2013). First, the ARBIMON analysis platform was used to transform each one-minute recording into a graphical representation of its spectral components, known as a spectrogram (constructed with 512 samples per temporal interval). Second, a supervised machine learning-based model (Aide et al., 2013) was applied to the entire volume of spectrograms to classify rain-contaminated spectrograms, which were removed to isolate the biotic contribution to the soundscape. Manual validation of the rainfall screening procedure (n = 100) yielded no false negatives and a precision of 0.93 (7% false positives). Third, the spectrograms collected at each site (n = 34) and during each day (n = 5) were aggregated by hour (24 h) and frequency (0–22 kHz; bin size: 344 Hz). For each of the constituent 1536 acoustic channels (24 h × 64 frequency bands), a binary detection history was generated based on an amplitude threshold of 0.02 (Aide et al., 2013). The resulting 3D matrix (x = hour, y = frequency, z = evidence of biotic activity) represented the synoptic signature of the acoustic community for each site and each daily survey.

2.4. Acoustic space occupancy model

We developed the ASOM framework to predict acoustic variability relevant to multiple taxa while accounting for biologically irrelevant variability due to observation bias. The model was adapted from the standard single season occupancy model (MacKenzie et al., 2002) to account for the fact that the occupancy status of an acoustic channel is not perfectly observable and that failure to detect acoustic space occupancy may result from inactivity of the constituent species or factors that limit signal propagation and detection (e.g. survey effort, sound attenuation).

Table 1
Lidar and ecoacoustic covariates evaluated for models of detection and occupancy. The only candidate covariates not fit to both model components were n and $(C_n + S_n)$, which were exclusively used as detection and observation covariates, respectively.

Data source	Covariates	Description
Lidar surveys	all_mean	Mean of all return heights (m)
	all_kurtosis	Kurtosis of all return heights (m)
	all_skewness	Skewness of all return heights (m)
	all_stdev	Standard deviation of all return heights (m)
	all_p10…all_p100	Height percentiles (10% increments) of all returns (m)
	tree_fract	Fraction of all returns classified as tree* (m)
	tree_fcover	Fraction of first returns intercepted by tree* (m)
	tree_iqr	Interquartile range (p75-p25) of returns classified as tree* (m)
	shrub_mean	Mean height of returns classified as shrub** (m)
	shrub_stdev	Standard deviation of return heights classified as shrub** (m)
	biomass	Aboveground carbon density (Mg C ha^{-1}) (Longo et al., 2016)
	residual_canopy	The percentage of the site with canopy heights ≥ intact reference (21 m) (Rappaport et al., 2018)
Acoustic surveys	freq	The frequency associated with a given transmission channel (Hz)
	n	Sample density, corresponding to the number of rain-free acoustic samples aggregated for each hour bin
	$(C_n + S_n)$	The sine–cosine pairs for the harmonic regression used to approximate the multimodal patterns in acoustic activity over a 24-hour period(n = 1: 4)

*Tree returns: returns > 1.37 *m*.
**Shrub returns: non-ground returns < 1.37 *m*.

Formally, let z_{ni} be the true occupancy status of acoustic channel n at sample location ("site") i. Each acoustic channel n is comprised of a frequency/time coordinate n = (f, t)such that n is analogous to a "site" in the classical occupancy modeling vernacular. Thus, acoustic channel n is the unit of occupancy in our study, whereas we use the term "site" to represent higher-level structure across which acoustic space occupancy might vary, such as a geographic stratum (e.g., forest patch), which is analogous to some type of blocking structure in classical occupancy modeling vernacular. Let y_{nik} denote the observed occupancy for acoustic channel n, site i, and sample occasion k.

Here, the five daily soundscapes (k = 1:5) for each site were treated as temporal replicate observations of each acoustic channel. We used a maximum likelihood estimation framework to build separate models for the observation process (i.e., acoustic space detection) and the true state process (i.e., acoustic space occupancy).

The true latent occupancy state of an acoustic channel (z_{ni}) can be modeled as a Bernoulli process described as:

$$z_{ni} \sim Bernoulli(\Psi_{ni}) \quad (1)$$

where Ψ_{ni} is the probability of occupancy of acoustic channel n at site i. We modeled the probability of occupancy as a function of covariates using a logistic model. For example, with a single covariate the model has the form:

$$\text{logit}(\Psi_{ni}) = \beta_0 + \beta_1 x_{ni} \quad (2)$$

where x_{ni} is a measured covariate that varies by dimensions of the acoustic soundscape (frequency and time) or varies across the different sample sites.

The observation process can be modeled as another Bernoulli random variable conditional on the state process:

$$y_{nik} \mid z_{ni} \sim Bernoulli(z_{ni} p_{nik}) \quad (3)$$

where y_{nik} is the realized detection of acoustic channel n at site i during survey k, and p_{nik} is the detection probability. We also modeled measured covariates on detection probability according to a logistic model, e.g., with one covariate:

$$\text{logit}(p_{nik}) = \alpha_0 + \alpha_1 x_{nik} \quad (4)$$

where x_{nik} is a measured covariate that varies by frequency, time of day, survey occasion or sample location.

We used Akaike's information criterion (AIC) to select the best-supported models for inference (Burnham & Anderson, 2003), and performed model selection stepwise. First, the top-ranked models (ΔAIC $\leq$ 2) were identified for the detection component, p, by assuming the null model for the occupancy component, Ψ. Then, the best-approximating models were identified for Ψ assuming the previously selected covariate set for p. The R program *unmarked* was used for ASOM model fitting and selection (R Development Core Team, 2018; Fiske & Chandler, 2011).

The ASOM framework allows covariate effects in the spectral or temporal dimensions of the soundscape, which can be used to model variability in either acoustic space occupancy or detection probability. In all candidate models, frequency was included either in linear or quadratic form as a fixed covariate for both Ψ and p to account for possible curvilinear effects of frequency-dependence on occupancy and sound transmission. Note that the frequency covariate (f) was transformed to facilitate model convergence (f-12/4 kHz) and models were fit to a frequency subset containing the central mass of the data (1.4–10 kHz) to avoid issues with data sparsity at the frequency extremes. Sample density (i.e. usable recordings per hour) was also included as a fixed covariate for p to account for detection bias due to variability in survey effort. Additionally, harmonic regression terms were used to model the multimodal peaks in occupancy from the diurnal periodicity in acoustic activity (Weir et al., 2005), estimated as:

$$\text{logit}(\Psi_{ni}) = \beta_0 + \beta_1 \cos\left(\frac{2\pi t f_c}{24}\right) + \beta_2 \sin\left(\frac{2\pi t f_c}{24}\right) \quad (5)$$

where β_1 and β_2 represent the sinusoidal amplitude and phase during the diurnal period, t represents the sampling time period, and f_c represents the frequency of the sinusoid, with up to 4 cycles per day (c = 1: 4) considered within each candidate model.

The ASOM framework also permits covariate effects to vary across the sites in which the soundscapes were observed. We used 22 lidar metrics to account for variability in forest structure across sites (Table 1). Covariate selection was guided by *a priori* hypotheses regarding the influence of habitat structure on biotic community assembly and signal attenuation, and our previous findings on the lidar metrics most useful for discriminating among complex Amazon forest structures (Longo et al., 2016; Rappaport et al., 2018). The lidar metrics were calculated using a 50 m radius from the location of the recording devices, and they were scaled and centered to assist with model convergence. We constructed candidate models with $\leq$2 lidar metrics for Ψ and p using an exhaustive model-fitting procedure (R package *MuMIN*; Barton, 2018), which evaluated linear combinations of predictors in the stepwise fashion described above. All variable pairs with Pearson correlation coefficients $\geq$0.6 were excluded from consideration to address potential issues with multicollinearity.

We evaluated three ecologically viable interactions among covariates selected in the top-ranked model: 1) An interaction between the lidar metrics and signal frequency in p to test the influence of habitat structure on frequency-dependent attenuation; 2) an interaction between the sinusoids and frequency in Ψ to account for the expected variability in diurnal activity across frequency bands (i.e. pseudo-taxa); and 3) an interaction between the lidar metrics and the sinusoids in Ψ to account for the hypothesized influence of 3D habitat structure on diurnal activity (i.e. from differences in community composition).

The model was calibrated with 33 of the 34 sites, and its predictive capacity was evaluated using cross validation with the remaining site. To assess classification accuracy, we calculated the area under the receiver operator curve at the site level (AUC) following Sadoti et al. (2013). AUC ranges from 0.5 to 1.0, and values above 0.80 indicate adequate discriminatory power.

Lastly, we used the top-supported model to generate predictions over the sampled range of degraded forest structures to support interpretation of covariate effects, as well as covariate ranges derived from the intact reference forests in the Xingu Indigenous Park to illustrate the utility of the ASOM framework for predicting outside of the immediate zone of study and forecasting conservation outcomes.

3. Results

There was substantial spectral-temporal variability in detected acoustic activity within and among the surveyed sites. The observed site-level proportion of occupied acoustic space, or 'naive' occupancy, ranged between 2 and 17% (mean: 7%). There was a marked influence of time of day on the observed utilization of frequency channels, and the diurnal patterning was not uniform across sites (Fig. 2). On average, naive occupancy was highest during the dusk to pre-dawn period (17:00–3:00), with detections progressively decreasing from a peak in activity during the dusk chorus. The largest gaps in utilized acoustic space were detected during the dawn to pre-dusk period (6:00–15:00) and only a small subset of sites contributed to aggregate detections at those hours (Fig. 2). On average, naive occupancy was highest at the middle frequencies (3–8 kHz) and lowest at the low (< 3 kHz) and high frequencies (> 8 kHz) (Fig. 3). At the high-frequency range, the relative proportion of detections in closed versus open forests progressively decreased with increasing frequency, and detections > 10 kHz were exclusively registered in degraded forests with open canopies (Fig. 3).

By accounting for the factors that influence signal detection, the ASOM framework permitted us to estimate latent soundscape structure

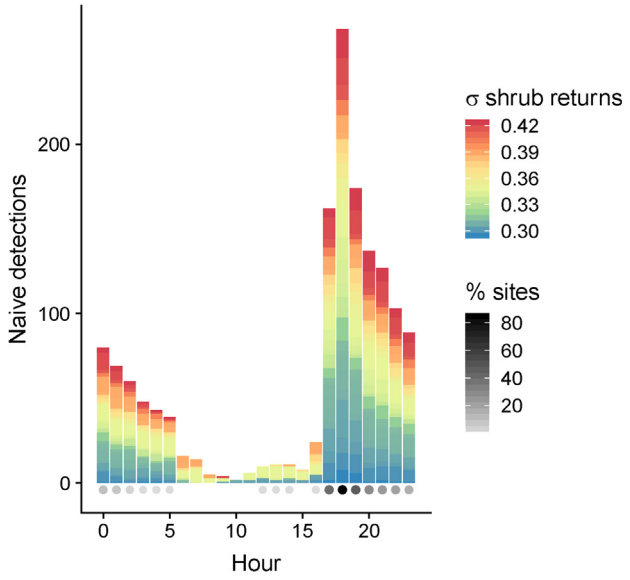

Fig. 2. Naive observations per hour for the 33 sites used for model calibration. Colors correspond to the degree of canopy openness of the corresponding sites (higher values of shrub standard deviation indicate greater canopy loss from degradation). The greyscale indicates the percentage of sites with ≥5 detections.

that would have otherwise been unobservable from the naive detections alone. The top-ranked model (Table 2) showed evidence of good predictive accuracy (AUC = 0.91), and results for the observation process (p) and state process (Ψ) model components will be presented in turn.

The sub-model for p revealed a strong frequency dependence of detection bias. The likelihood of detecting acoustic activity peaked around 5 kHz, and was governed by a quadratic effect of frequency (Fig. 4). The requisite sampling effort needed to maximize p also varied as a function of frequency, and high frequencies were predicted as being most susceptible to detection failure regardless of sample density (Fig. 5). In an average forest, the likelihood of detecting the lowest, average, and highest frequency bands was 8%, 39% and 1%, respectively, assuming maximum temporal coverage from our study design (12 samples/hour). At the most intensive sampling protocol theoretically possible (60 samples/hour), it increased to 77%, 96%, and 21%, respectively.

Our frequency-dependent predictions of detection probability were improved by including estimates of forest structure to account for signal interference with vegetation. Two lidar covariates were selected in the

Table 2
The model with the most substantial level of empirical support is shown with coefficients (SE) presented separately for the detection and occupancy components. Covariate descriptions are provided in Table 1.

Probability of acoustic space detection	
$Y_{nik}(*)\rho_{nik}(freq^2 + n + biomass + shrub\_stdev)$	
Intercept	−10.08 (0.35)
biomass	0.46 (0.03)
freq	−9.87 (0.47)
$freq^2$	−2.75 (0.15)
n	0.07 (0.01)
shrub_stdev	0.13 (0.03)
Probability of acoustic space occupancy	
$\Psi_{ni}(freq \bullet (C_1 + S_1 + C_2 + S_2 + C_3 + S_3 + C_4 + S_4) \bullet tree\_fract + shrub\_stdev^2)$	
Intercept	−4.69 (0.41)
shrub_stdev	−0.07 (0.05)
$shrub\_stdev^2$	0.24 (0.04)
C_1	1.93 (0.53)
C_2	−1.75 (0.47)
C_3	−0.69 (0.48)
C_4	1.27 (0.34)
S_1	−4.96 (0.51)
S_2	−1.62 (0.52)
S_3	1.72 (0.44)
S_4	−0.89 (0.35)
tree_fract	−1.59 (0.44)
freq	−0.81 (0.21)
C_1:tree_fract	−0.88 (0.76)
C_2:tree_fract	1.09 (0.60)
C_3:tree_fract	0.69 (0.49)
C_4:tree_fract	0.49 (0.39)
S_1:tree_fract	0.73 (0.48)
S_2:tree_fract	0.58 (0.48)
S_3:tree_fract	0.57 (0.46)
S_4:tree_fract	−1.25 (0.40)
C_1:freq	0.07 (0.26)
C_2:freq	−0.67 (0.23)
C_3:freq	−0.18 (0.23)
C_4:freq	0.47 (0.17)
S_1:freq	−1.87 (0.24)
S_2:freq	−0.87 (0.25)
S_3:freq	0.73 (0.22)
S_4:freq	−0.36 (0.17)
tree_fract:freq	−0.58 (0.23)
C_1:tree_fract:freq	−0.23 (0.39)
C_2:tree_fract:freq	0.29 (0.31)
C_3:tree_fract:freq	0.52 (0.25)
C_4:tree_fract:freq	0.17 (0.20)
S_1:tree_fract:freq	0.49 (0.24)
S_2:tree_fract:freq	0.31 (0.24)
S_3:tree_fract:freq	0.19 (0.24)
S_4:tree_fract:freq	−0.49 (0.21)

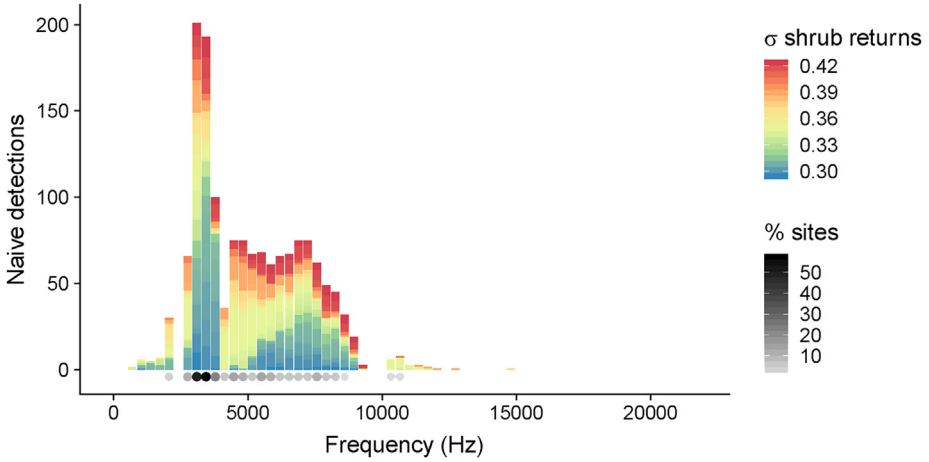

Fig. 3. Naive observations per frequency band. Colors correspond to the degree of canopy openness and the greyscale corresponds to the percentage of sites with ≥5 detections.

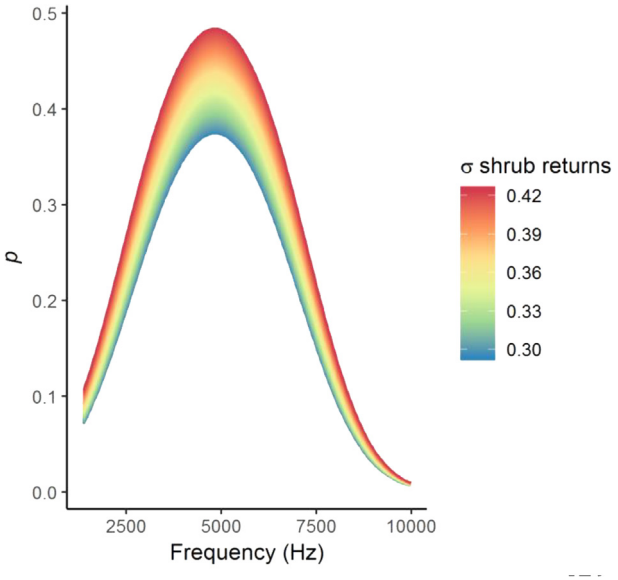

Fig. 4. The combined effects of signal frequency and forest structure, indicated by the standard deviation of shrub-classified lidar returns, on top-ranked model predictions of detection probability (p), assuming 12 samples/hour and mean values for other detection covariates (not shown).

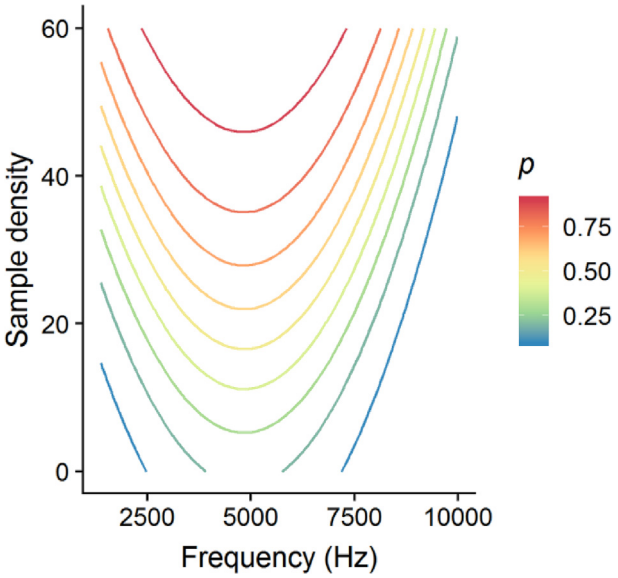

Fig. 5. The influence of sample density on frequency-dependent detection probability (p) predicted from the top-ranked model, assuming average forest characteristics and a maximum sample density of 60 one-minute recordings per hour.

top-ranked model for p, aboveground biomass and the standard deviation of shrub heights (Table 2). When predicted over the entire sampled distribution of degraded forest structure, maximum estimates of p increased compared to the estimates above, exceeding 60% for the lowest, average, and highest frequency channels (assuming sample density of 12 recordings/hour). In each case, maximum p was predicted for heavily degraded forests that ranked in the top 10th percentile of sampled shrub standard deviation, a lidar metric that indicates more heterogeneous vegetation cover from 0 to 1.3 m, typical of degraded Amazon forests with low fractional tree cover. This suggests that acoustic signals were more readily detectable in heavily altered and open forest environments (Fig. 4).

Forest structure was also important for explaining variation in

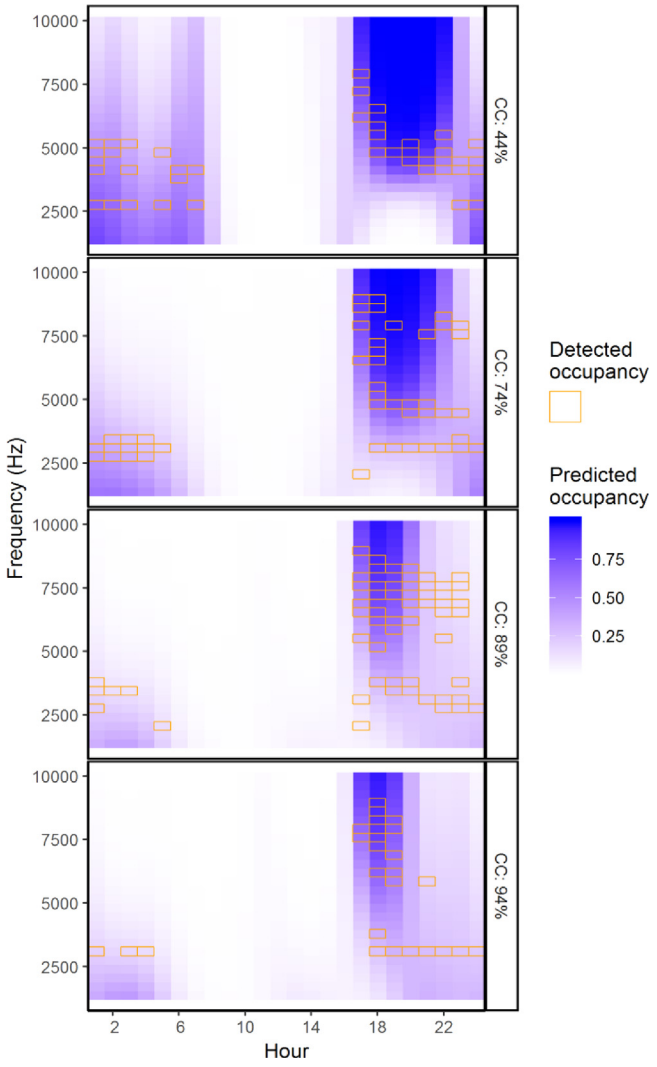

Fig. 6. Predicted occupancy (blue scale) overlaid with naive detected occupancy aggregated over five days (orange outline) for four study sites with differing fractional canopy cover (CC).

acoustic space occupancy. Based on model selection of the state process component (Table 2), variability in Ψ was best approximated by a three-way interaction between four sinusoids, frequency, and the lidar-derived covariate, tree fractional cover, which allowed the diurnal patterns of acoustic activity to vary across the frequency and habitat domains. The top-ranked model also included shrub standard deviation as a quadratic effect, which further constrained variability in Ψ as a function of forest structure. Patterns of predicted and observed occupancy were in close agreement over the sampled habitat distribution. In most cases, transmission channels that were predicted as having a high likelihood of occupancy were also registered by the acoustic surveys (Fig. 6). Divergence between modeled and observed occupancy occurred primarily for predictions in dense forest conditions and frequency bands estimated as most vulnerable to attenuation (Figs. 3, 6).

Estimates of Ψ revealed a diversity of acoustic community assemblages with distinct occupancy patterns across the time and frequency domains, and notable differences between intact and degraded habitats. When predicted for the average degraded forest and mean frequency, the largest peak in Ψ (mean acoustic space occupancy: 56%) occurred during the early evening hours of the insect chorus (18:00–19:00) (Fig. 7). The diurnal peaks in acoustic activity varied within each frequency channel. Often, the low and high frequencies had contrasting patterns of occupancy. For example, within the same two-hour time

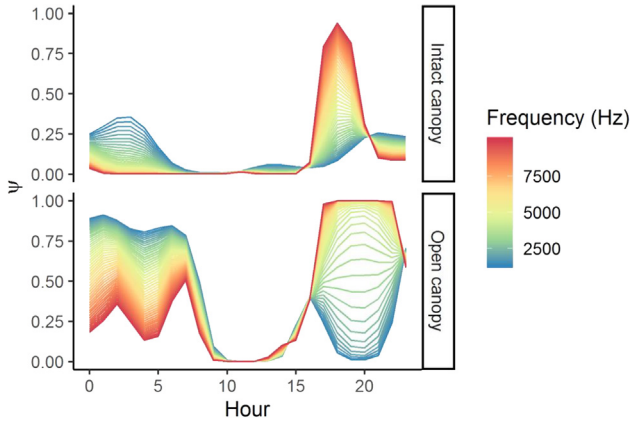

Fig. 7. Predicted occupancy probability (Ψ) over the 24-hour cycle and frequency spectrum for two divergent habitats, a heavily degraded forest (44% canopy cover), and an intact forest (93% canopy cover).

interval associated with the onset of the insect chorus, acoustic space occupancy ranged between 7% and 97% in the lowest and highest frequency channels, respectively. The opposite dynamic was observed for the pre-dawn/dawn period (24:00–7:00), during which low frequencies predominated (33%) and high frequencies were virtually absent (1%). The differences in model predictions between intact and degraded forest habitats were large, particularly for the same two contrasting time intervals (Figs. 6 and 7). For example, estimates of Ψ during the pre-dawn/dawn period (24:00–7:00) ranged between 23% and 85% for the most utilized frequency channel (1.4 kHz), depending on whether canopy structure was closed or open, respectively (Fig. 7).

4. Discussion

We developed a flexible methodological framework for capturing biologically plausible variation in acoustic quantities while accounting for sampling artifacts and failure in detecting animal-generated signals. Application of ASOM to a complex tropical forest mosaic illustrated four key attributes of our analytic framework. First, in assuming that the true underlying acoustic community is an unobservable structure, ASOM provides a clear coherent linkage between the observed soundscape and the true latent soundscape, the object of inference. Second, the flexible hierarchical structure of our modeling framework allows the factors that govern the ecological process and the observation process to be modeled separately. We provide clear evidence that the likelihood of detecting biotic signals varies across degraded forest environments, which could otherwise confound inferences about the legacy of habitat degradation on biodiversity. Third, by retaining the multidimensional structure of the community-level acoustic signature, ASOM captures multiple taxa, even in tropical forests where sonic space is shared by simultaneous biotic signals and noisy abiotic processes. Lastly, ASOM provides a flexible framework for predicting the assemblage of acoustic communities, and we demonstrate its use for making predictions for intact forests beyond the sampled distribution of degraded habitats and for populating data-poor regions of the soundscape.

Hierarchical models that combine 3D observations of physical space filling and acoustic space filling provide a path forward for handling detection bias in soundscape studies. Existing analysis methods regard soundscapes as unbiased representations of the underlying animal community, yet soundscapes are intrinsically imperfect and vulnerable to the same issues of detection bias that affect species distribution modeling in general (e.g., MacKenzie et al., 2002). Even within an individual site, there are important sources of detection heterogeneity, including minor variations in the expression of biotic signals over time (e.g. weather, phenology, etc.). Fortunately, multi-day soundscape surveys capture temporal heterogeneity by design, and hierarchical occupancy models are uniquely equipped to model the effects responsible for observed heterogeneity. Our hierarchical framework also provides estimates of between-site detection heterogeneity. By drawing upon the synergies between ecoacoustics and airborne lidar to capture aspects of the physical interactions between sound and structure, our empirical predictions of frequency-dependent detection failure were consistent with expectations from physics. We estimated that the risk of detection failure was greatest for high frequencies (> 8 kHz), slightly lower for low frequencies (< 3 kHz), and lowest for middle frequencies (3–8 kHz), similar to physical models of the forested environment that account for sound attenuation from interference with vegetation and ground (e.g. Wiley & Richards, 1982). It is not surprising, then, that the mode of our naive observations was in the most-detectable middle-frequency zone, or that the majority of our high-likelihood predictions that were not registered by our recorders were in the high-frequency zone, which is most vulnerable to attenuation from scattering (Wiley & Richards, 1982). Similarly, only samples from heavily degraded sites with only a few trees remaining to scatter sound contained detections with frequencies above 10 kHz. It should be noted that scattering is also caused by non-stationary heterogeneities (e.g., atmospheric turbulence), which mediate the effect of habitat on sound transmission (Wiley & Richards, 1982) and cannot be captured by lidar alone, but could perhaps be better approximated with physical models of acoustic attenuation. Signal transmission may also be better parameterized with alternative estimates of the structural environment, such as tree diameter distributions retrievable from terrestrial laser scanning or forest inventory data.

Formalized procedures for characterizing uncertainty, such as the ASOM framework, also provide a means to guide sampling effort allocation and adjust for data sparsity. We demonstrated the utility of our model for informing study design by predicting detection uncertainties over a range of sampling protocols. For example, we estimated that in an average forest, the probability of detecting acoustic activity in the least detectable frequency channel would not exceed 10%, even when increasing sample density to 50% daily coverage, a probability which may or may not be considered adequate depending on the uncertainty thresholds and objectives of the monitoring program in question. Optimizing predictive power amidst resource constraints requires a clear understanding of sampling tradeoffs (e.g. spatial vs. temporal replicates). Hierarchical occupancy models are uniquely suited to inform such assessments through simulation-based exercises (Bailey et al., 2007). Further, as acoustic monitoring networks expand in scale (Gibb et al., 2019), there will be an increasing need to obtain accurate confidence intervals on ecological inferences derived from sparse and complicated ecoacoustic datasets.

Since the multidimensional soundscape reflects the taxonomic complexity of the biodiversity process (Aide et al., 2017), its constituent 'channels' may offer sufficient resolution for monitoring change. Assessing differences between soundscapes (β diversity) is even more challenging than estimating biodiversity within soundscapes, and the current set of β-diversity methods require perfect homologies that are often impractical, even for simultaneous recordings (Sueur et al., 2014), and readily confounded by environmental variation and noise (Buxton et al., 2018). By abstracting the soundscape into a map of spectral-temporal transmission channels, our analytic framework permitted us to model differences between biotic community assemblages across a complex forest landscape mosaic with variable sources of background noise and signal interference. Since the coarseness of the channels and number of diurnal replicates are effectively model assumptions, exploring the synoptic scale of the soundscape to address underlying heterogeneity should be a logical extension of this work. Targeting soundscape regions that represent peak activity of particular taxa could also be informative and possibly more tractable than modeling the full diurnal signal. Our findings from disaggregating the community-level response curves suggest that the signal of Amazon forest degradation may be most evident in the transmission channels predominantly

occupied by insects (e.g. midnight), warranting targeted investigations into their potential role as acoustic indicators of habitat change.

We anticipate a range of methodological developments to extend the applicability of the ASOM framework. A Bayesian implementation could allow for greater flexibility in capturing the fine-scale structure and dependencies in time–frequency space than what can be approximated with sinusoidal functions and low-order polynomials. A Bayesian framework would more easily allow for flexible spatial surface modeling using GAMs (Carroll et al., 2010) or computationally efficient methods used in high-dimensional space–time applications such as Empirical Orthogonal Functions (EOFs, Wikle & Cressie, 1999). More sophisticated techniques could be used to adjust for the abiotic occupancy of acoustic space, including Poisson processes to differentiate true and false positives from continuous detection information on the Z-axis (e.g. Chambert et al., 2018). Moreover, collapsing the Z-axis into binary presence-absence values, as required by the traditional binomial model, may not be the most efficient use of the 3D soundscape. For example, the relative abundance of soundscape quantities could be used with N-mixture models (e.g. Royle, 2004) to investigate how metapopulation dynamics are reflected in acoustic assemblages. Lastly, the ASOM framework could also be readily extended to track longitudinal dynamics (e.g. MacKenzie et al., 2003).

5. Conclusion

Ecoacoustics represents an exciting pathway for routine biodiversity monitoring on the scale needed to support the derivation of essential biodiversity variables (EBVs). Yet, its operational potential depends on statistical solutions for characterizing multiple taxa, handling data complexity, and addressing observation bias—methodological criteria that have proven most challenging in biodiverse tropical forests (Eldridge et al., 2018; Gibb et al., 2019). By applying our analytic framework to a dynamic Amazon forest frontier, we show its potential for meeting these objectives while addressing knowledge gaps from chronically under-sampled taxa, such as insects. Our findings also underscore important synergies between lidar and ecoacoustics for informing models of occupancy and detection, and supporting future investigations into the role of habitat structure in shaping habitat use. Our flexible framework can be readily extended to other forest types and regional contexts to account for observation bias from imperfect detection of forest pseudo-taxa likely to be affected by sound attenuation.

6. Authors' contributions

DIR, JAR, and DCM collaborated in the conception of the research ideas and development of the methodology; DIR acquired and analyzed the data, and led the writing of the manuscript. All authors made substantial contributions to the writing process and approved submission of this manuscript for publication.

Acknowledgements

Support was provided by the NASA Earth and Space Science Fellowship program (D. I. Rappaport), a National Science Foundation Doctoral Dissertation Research Improvement Grant (D. I. Rappaport, grant 1634168), and NASA's Carbon Monitoring System program. Sustainable Landscapes Brazil collected the lidar data, and Maiza Dos-Santos and Hyeungu Choi provided assistance with data processing. We also thank biologist Eveline Salvático for her valuable support in the field during acoustic data collection.

Data accessibility

The lidar data are accessible from: http://mapas.cnpm.embrapa.br/paisagenssustentaveis/.

References

Aide, T.M., Corrada-Bravo, C., Campos-Cerqueira, M., Milan, C., Vega, G., Alvarez, R., 2013. Real-time bioacoustics monitoring and automated species identification. PeerJ 1, e103. https://doi.org/10.7717/peerj.103.

Aide, T.M., Hernández-Serna, A., Campos-Cerqueira, M., Acevedo-Charry, O., Deichmann, J.L., 2017. Species richness (of insects) drives the use of acoustic space in the tropics. Remote Sens. 9 (11), 1096. https://doi.org/10.3390/rs9111096.

Bailey, L.L., Hines, J.E., Nichols, J.D., MacKenzie, D.I., 2007. Sampling design trade-offs in occupancy studies with imperfect detection: examples and software. Ecol. App. 17 (1), 281–290.

Barton, K. (2018). Package 'MuMIn'. R package version 1.40. 4.

Bergen, K. M., Goetz, S. J., Dubayah, R. O., Henebry, G. M., Hunsaker, C. T., Imhoff, M. L., … Radeloff, V. C. (2009). Remote sensing of vegetation 3-D structure for biodiversity and habitat: Review and implications for lidar and radar spaceborne missions. Journal of Geophysical Research: Biogeosciences, 114(G2), n/a–n/a. doi:10.1029/2008JG000883.

Burnham, K.P., Anderson, D.R., 2003. Model Selection and Multimodel Inference: A Practical Information-Theoretic Approach. Springer Science & Business Media.

Bush, A., Sollmann, R., Wilting, A., Bohmann, K., Cole, B., Balzter, H., Yu, D.W., 2017. Connecting earth observation to high-throughput biodiversity data. Nat. Ecol. Evol. 1 (7), 0176. https://doi.org/10.1038/s41559-017-0176.

Buxton, R.T., McKenna, M.F., Clapp, M., Meyer, E., Stabenau, E., Angeloni, L.M., Wittemyer, G., 2018. Efficacy of extracting indices from large-scale acoustic recordings to monitor biodiversity. Conserv. Biol. 32 (5), 1174–1184. https://doi.org/10.1111/cobi.13119.

Cardinale, B.J., Duffy, J.E., Gonzalez, A., Hooper, D.U., Perrings, C., Venail, P., Naeem, S., 2012. Biodiversity loss and its impact on humanity. Nature 486 (7401), 59–67. https://doi.org/10.1038/nature11148.

Carroll, C., Johnson, D.S., Dunk, J.R., Zielinski, W.J., 2010. Hierarchical bayesian spatial models for multispecies conservation planning and monitoring. Conserv. Biol. 24 (6), 1538–1548.

Chambert, T., Waddle, J.H., Miller, D.A., Walls, S.C., Nichols, J.D., 2018. A new framework for analysing automated acoustic species detection data: Occupancy estimation and optimization of recordings post-processing. Methods Ecol. Evol. 9 (3), 560–570.

Cook, B.D., Nelson, R.F., Middleton, E.M., Morton, D.C., McCorkel, J.T., Masek, J.G., et al., 2013. NASA Goddard's LiDAR, Hyperspectral and Thermal (G-LiHT) Airborne Imager. Remote Sens. 5 (8), 4045–4066.

Eldridge, A., Casey, M., Moscoso, P., Peck, M., 2016. A new method for ecoacoustics? Toward the extraction and evaluation of ecologically-meaningful soundscape components using sparse coding methods. PeerJ 4, e2108. https://doi.org/10.7717/peerj.2108.

Eldridge, A., Guyot, P., Moscoso, P., Johnston, A., Eyre-walker, Y., Peck, M., 2018. Sounding out ecoacoustic metrics: avian species richness is predicted by acoustic indices in temperate but not tropical habitats. Ecol. Indic.

Fiske, I., Chandler, R., 2011. Unmarked: an R package for fitting hierarchical models of wildlife occurrence and abundance. J. Stat. Software 43 (10), 1–23.

Gibb, R., Browning, E., Glover-Kapfer, P., Jones, K.E., 2019. Emerging opportunities and challenges for passive acoustics in ecological assessment and monitoring. Methods Ecol. Evol. 10 (2), 169–185.

Goetz, S., Steinberg, D., Dubayah, R., Blair, B., 2007. Laser remote sensing of canopy habitat heterogeneity as a predictor of bird species richness in an eastern temperate forest, USA. Remote Sens. Environ. 108 (3), 254–263. https://doi.org/10.1016/j.rse.2006.11.016.

Krause, B., 1987. Bioacoustics, habitat ambience in ecological balance. Whole Earth Rev. 57, 14–18.

Longo, M., Keller, M.M., dos-Santos, M.N., Leitold, V., Pinagé, E.R., Baccini, A., Morton, D.C., 2016. Aboveground biomass variability across intact and degraded forests in the Brazilian Amazon. Global Biogeochem. Cycles. https://doi.org/10.1002/2016GB005465. 2016GB005465.

MacKenzie, D.I., Nichols, J.D., Hines, J.E., Knutson, M.G., Franklin, A.B., 2003. Estimating site occupancy, colonization, and local extinction when a species is detected imperfectly. Ecology 84 (8), 2200–2207.

MacKenzie, D.I., Nichols, J.D., Lachman, G.B., Droege, S., Andrew Royle, J., Langtimm, C.A., 2002. Estimating site occupancy rates when detection probabilities are less than one. Ecology 83 (8), 2248–2255.

MacKenzie, D.I., Nichols, J.D., Andrew Royle, J., Pollock, K.H., Bailey, L.L., Hines, J.E., 2018. Occupancy in community-level studies. In: Occupancy Estimation and Modeling. Elsevier, pp. 557–583. https://doi.org/10.1016/B978-0-12-407197-1.00020-X.

Meyer, C., Kreft, H., Guralnick, R., Jetz, W., 2015. Global priorities for an effective information basis of biodiversity distributions. Nature Comm. 6, 8221. https://doi.org/10.1038/ncomms9221.

Pekin, B.K., Jung, J., Villanueva-Rivera, L.J., Pijanowski, B.C., Ahumada, J.A., 2012. Modeling acoustic diversity using soundscape recordings and LIDAR-derived metrics of vertical forest structure in a neotropical rainforest. Landscape Ecol. 27 (10), 1513–1522.

Pijanowski, B.C., Villanueva-Rivera, L.J., Dumyahn, S.L., Farina, A., Krause, B.L., Napoletano, B.M., Pieretti, N., 2011. Soundscape ecology: the science of sound in the landscape. BioScience 61 (3), 203–216. https://doi.org/10.1525/bio.2011.61.3.6.

Rappaport, D.I., Morton, D.C., Longo, M., Keller, M., Dubayah, R., dos-Santos, M. N., 2018. Quantifying long-term changes in carbon stocks and forest structure from Amazon forest degradation. Environ. Res. Lett. 13 (6), 065013. https://doi.org/10.1088/1748-9326/aac331.

R Core Team, 2018. A language and environment for statistical computing. R Foundation

for Statistical Computing, Vienna, Austria. URL https://www.R-project.org/.
Robinson, W.D., Lees, A.C., Blake, J.G., 2018. Surveying tropical birds is much harder than you think: a primer of best practices. Biotropica.
Royle, J.A., 2004. N-Mixture models for estimating population size from spatially replicated counts. Biometrics 60 (1), 108–115. https://doi.org/10.1111/j.0006-341X.2004.00142.x.
Royle, J.A., 2018. Modelling sound attenuation in heterogeneous environments for improved bioacoustic sampling of wildlife populations. Methods Ecol. Evol. 9 (9), 1939–1947. https://doi.org/10.1111/2041-210X.13040.
Sadoti, G., Zuckerberg, B., Jarzyna, M.A., Porter, W.F., 2013. Applying occupancy estimation and modelling to the analysis of atlas data. Divers. Distrib. 19 (7), 804–814.
Sueur, J., Farina, A., Gasc, A., Pieretti, N., Pavoine, S., 2014. Acoustic indices for biodiversity assessment and landscape investigation. Acta Acustica United with Acustica 100 (4), 772–781.
Troudet, J., Grandcolas, P., Blin, A., Vignes-Lebbe, R., & Legendre, F. (2017). Taxonomic bias in biodiversity data and societal preferences. Scientific Reports, 7(1), 9132. doi:10.1038/s41598-017-09084-6.
Weir, L.A., Royle, J.A., Nanjappa, P., Jung, R.E., 2005. Modeling anuran detection and site occupancy on North American Amphibian Monitoring Program (NAAMP) routes in Maryland. J. Herpetol. 39 (4), 627–639.
Wikle, C.K., Cressie, N., 1999. A dimension-reduced approach to space-time Kalman filtering. Biometrika 86 (4), 815–829.
Wiley, R.H., Richards, D.G., 1982. Adaptations for acoustic communication in birds: sound transmission and signal detection. In: Kroodsma, D., Miller, E.H., Ouellet, H. (Eds.), Acoustic Communication in Birds. Academic Press, New York, pp. 131–181.